UDC 621.313.3

MAXIMUM POWER EXTRACTION FROM SELF-EXCITED INDUCTION GENERATORS

O. Kiselychnyk, J. Wang
University of Warwick
Coventry, CV4 7AL, United Kingdom. E-mail: O.Kiselychnyk@warwick.ac.uk, jihong.wang@warwick.ac.uk
M. Bodson
University of Utah
Salt Lake City, UT 84112, USA. E-mail: bodson@eng.utah.edu
M. Pushkar
National Technical University of Ukraine "Kyiv Polytechnic Institute"
prosp. Peremohy, 37, Kyiv, 03056, Ukraine. E-mail: pushkar.mykola@gmail.com

Technologies for voltage control of self-excited induction generators can also be applied for maximum power extraction in specific applications without strict restrictions on the generated frequency and voltage. The main problem in designing such systems is the lack of appropriate theoretical analysis. The paper considers an approach for maximizing the power extracted from self-excited induction generators. It derives formulas for the steady-state generated power and self-excitation boundaries. Since an analytic search for a maximum of the power as a function of capacitance and load admittance is impossible, a numerical approach including 3-D computational and 2-D experimental results is used to show the existence of a global maximum of the power for a specific velocity in the capacitance - load admittance plane and within the self-excitation boundary. Therefore, the method allows one to take into account all possible operating points for this velocity. The implementation of maximum searching algorithms is discussed.

Key words: induction generator, self-excitation, maximum extracted power, steady-state power characteristics.

ГЕНЕРУВАННЯ МАКСИМАЛЬНОЇ ПОТУЖНОСТІ АСИНХРОННИХ ГЕНЕРАТОРІВ ІЗ САМОЗБУДЖЕННЯМ

О. І. Кіселичник, Дж. Вонг
Університет Ворвіка
Ковентрі, CV4 7AL, Великобританія. E-mail: O.Kiselychnyk@warwick.ac.uk, jihong.wang@warwick.ac.uk
М. Бодсон
Університет Юти
Солт Лейк Сіті, UT 84112, США. E-mail: bodson@eng.utah.edu
М. В. Пушкар
Національний технічний університет України "Київський політехнічний інститут"
просп. Перемоги, 37, м. Київ, 03056, Україна. E-mail: pushkar.mykola@gmail.com

Способи керування напругою асинхронних генераторів із самозбудженням можуть бути використані для максимізації потужності окремих застосувань, що не мають жорстких вимог щодо генерованої частоти та напруги. Основною проблемою розробки таких систем є відсутність відповідних теоретичних основ. У роботі розглядається підхід щодо максимізації генерованої потужності асинхронних генераторів із самозбудженням. Отримуються вирази для статичної потужності генератора й границь самозбудження. Оскільки аналітичне дослідження залежності потужності від ємності конденсаторів та провідності навантаження на екстремум виявляється неможливим, то застосовується числовий метод, який включає побудову тривимірних розрахункових і двовимірних експериментальних характеристик, що доводять існування точки глобального максимуму потужності в межах границі самозбудження для відповідної швидкості, побудованої в площині ємність–провідність навантаження. Таким чином, даний метод дозволяє врахувати всі можливі робочі точки генератора для даної швидкості. Дискутується питання реалізації алгоритмів пошуку точки максимуму потужності.

Ключові слова: асинхронний генератор, самозбудження, максимальна вихідна потужність, статичні характеристики потужності.

PROBLEM STATEMENT. Self-excited induction generators (SEIG) have found applications in stand-alone power generation for remote areas without grid supply lines. The main problem of SEIGs is voltage and frequency deviations with changes of the load. Therefore, different voltage control technologies are developed to satisfy the needs of consumers [1, 2]. Mainly, they are based on dump load or capacitance regulation [3–9], or injection of capacitive currents through static synchronous compensators, or voltage or current source inverters [10–14]. The proposed systems mainly concern the problem of voltage stabilization and focus on control technologies for implementations. They don't address the question of possible maximum SEIG power extraction. For specific types of loads, like heating or lighting systems, systems with SEIGs output AC–DC conversion, for which there are no strict requirements concerning voltage and frequency, the maximum power extraction could be provided via control methods applied for the voltage regulation. The objective of the paper is to provide a theoretical framework for such control, including a demonstration of the existence of a maximum power operating point and recommendations for implementation of an optimal control algorithm.

The solution of this problem was hindered by the fact that till the recent time there were no equations (formulas) presented in the literature which would state an explicit dependence between SEIG generated power and load, including possible control actions such as capacitance and velocity, that would allow one to search for maximum point either analytically or via computations of all possible operating points. The origin of the problem was that the steady-state SEIG voltages were computed based on a system of two polynomial equations (or equivalent one polynomial) accounting for nonlinearity of magnetic saturation via iterative methods for each operating point [15–19]. These computations provided valid results only for specific regions where self-excitation sustains (self-excitation boundaries). The computation of the boundaries (or self-excitation conditions, critical capacitance, velocity and load) was also performed similar to the computation of the steady states based on polynomials derived from equating to zero either the total loop impedance [18, 20, 21] or the total node admittance at the magnetizing branch [22–24]. The generalized two-phase model of the induction machine was also used to search for parameters such that the system of differential equations describing the SEIG becomes unstable around the zero state [19, 25–27]. In such a manner in both the cases only specific points belonging to the self-excitation boundaries were computed not showing the whole shapes of the curves and consuming a lot of time for computations of some extended regions of capacitance and velocity. It allowed computing power in these regions and search numerically for some possible local maximum.

The approach proposed in the paper is based on recent results of the authors obtained due to derivation of an analytical steady-state solution of the system of the differential equations describing the SEIG. Considering the steady-state SEIG model with complex variables yielded explicit formulas for steady-state voltages and self-excitation boundaries allowing to compute the whole curves without iterations [28–30]. The paper derives the formula for steady state power as a function of generated frequency, magnetizing inductance, capacitance, and load admittance. Since the generated frequency can't be explicitly found from a polynomial of the fifth order with parameters depending on the capacitance and load admittance, and the magnetizing inductance depends on the frequency, capacitance and load admittance, then the analytical search for maximum point of the power function appears to be impossible.

An alternative numerical approach is used. For given value of the velocity, the self-excitation boundary is determined in the capacitance – load admittance plane, while typically in the literature only self-excitation boundaries in the velocity – capacitance plane are considered. This boundary determines all possible pairs of capacitance and load for which self-excitation exists. Then computation of power for all operating points within the self-excitation boundary allows to plot 3–D dependence of power on capacitance and load admittance and to show the existence of a global power maximum for given velocity. The results of computations are verified by experimental dependences of the generated power on load admittance for given velocities, and on velocity for given loads. For more generalization, two different induction machines are researched produced in Ukraine and UK. Possible control algorithm for maximum power search is discussed.

EXPERIMENTAL PART AND RESULTS OBTAINED. A two-phase model of SEIG with resistive loads and capacitors placed in parallel with the stator winding is considered in an arbitrary rotating F-G reference frame accounting for magnetic saturation [28], [31]

$$E\dot{X} = FX\,, \tag{1}$$

where $X = \left[U_{SF}\ i_{SF}\ i_{RF}\ U_{SG}\ i_{SG}\ i_{RG}\right]^T$;

$$F = \begin{bmatrix} F_1 & -F_2 \\ F_2 & F_1 \end{bmatrix},\ E = \begin{bmatrix} E_F & E_{FG} \\ E_{FG} & E_G \end{bmatrix},\ F_1 = \begin{bmatrix} Y_L & 1 & 0 \\ 1 & -R_S & 0 \\ 0 & 0 & -R_R \end{bmatrix};$$

$$F_2 = \begin{bmatrix} C\omega_e & 0 & 0 \\ 0 & -\omega_e(L_{\sigma S}+L_M) & -\omega_e L_M \\ 0 & \left(n_p\omega-\omega_e\right)L_M & \left(n_p\omega-\omega_e\right)(L_{\sigma R}+L_M) \end{bmatrix};$$

$$E_F = \begin{bmatrix} -C & 0 & 0 \\ 0 & L_{\sigma S}+L_{MF} & L_{MF} \\ 0 & L_{MF} & L_{\sigma R}+L_{MF} \end{bmatrix};$$

$$E_{FG} = \begin{bmatrix} 0 & 0 & 0 \\ 0 & L_{MFG} & L_{MFG} \\ 0 & L_{MFG} & L_{MFG} \end{bmatrix};$$

$$E_G = \begin{bmatrix} -C & 0 & 0 \\ 0 & L_{\sigma S}+L_{MG} & L_{MG} \\ 0 & L_{MG} & L_{\sigma R}+L_{MG} \end{bmatrix}.$$

In (1), U_{SF}, U_{SG}, i_{SF}, i_{SG} denote the F and G components of the stator voltages and currents, respectively, i_{RF}, i_{RG} denote the components of the rotor currents, ω_e is the angular velocity of the reference frame, $Y_L = 1/R_L$ is the admittance of the resistive load, C is the value of the capacitor, ω is the angular velocity of the rotor, R_S and R_R are the stator and rotor resistances, $L_{\sigma S}$ and $L_{\sigma R}$ denote the stator and rotor leakage inductances, and n_p is the number of pole pairs. The magnetizing inductance $L_M = f(i_M)$ is a static function of the amplitude of the magnetizing current (Fig. 1) while L_{MF}, L_{MG} and L_{MFG} are inductances caused by cross-saturation effects and are functions of L_M and components of the magnetizing currents.

$$L_{MF} = L_M + (L - L_M)i_{MF}^2 / i_M^2\,;$$
$$L_{MG} = L_M + (L - L_M)i_{MG}^2 / i_M^2\,;$$
$$L_{MFG} = (L - L_M)i_{MF}i_{MG} / i_M^2\,, \tag{2}$$

where $L = d\Psi_M / di_M = L_M + i_M dL_M / di_M$ denotes the dynamic magnetizing inductance, $i_M = \sqrt{i_{MF}^2 + i_{MG}^2}$.

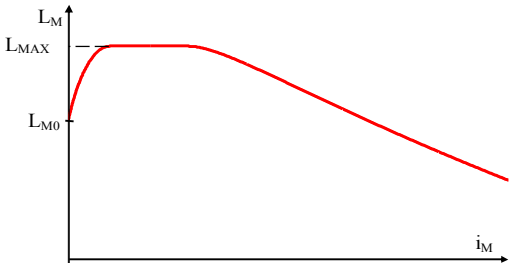

Figure 1 – Dependence of magnetizing inductance on magnetizing current

Follow the approach from [28] to derive the formula for the steady state generated power.

For steady state $FX = 0$. Then self-excitation corresponds to the existence of a frequency ω_e^* and a non-zero steady state vector X^* such that

$$F^* X^* = 0, \tag{3}$$

where F^* is the function F evaluated at the L_M^* corresponding X^*. The equation can be presented in a complex form

$$\left(F_1^* + jF_2^*\right) Z^* = 0, \tag{4}$$

where $Z^* = X_1^* + jX_2^*$; $X^* = \left[X_1^* \;\; X_2^*\right]^T$.

A non-zero solution of (4) exists only if

$$\det(F_1^* + jF_2^*) = 0. \tag{5}$$

The real and imaginary parts of (5) yield two equations the simultaneous solution of which gives polynomial equation for the generated frequency

$$\begin{aligned} &C^2\left(R_S L_{\sigma R}^2 + R_R L_{\sigma S}^2\right)\omega_e^{*5} - n_p \omega C^2\left(2R_S L_{\sigma R}^2 + R_R L_{\sigma S}^2\right)\omega_e^{*4} + \\ &+\left(\left(n_p\omega\right)^2 C^2 R_S L_{\sigma R}^2 + C^2 R_R^2 R_S + C^2 R_R R_S^2 - 2CR_R L_{\sigma S} + \right. \\ &\left. +Y_L^2 R_S L_{\sigma R}^2 + Y_L L_{\sigma R}^2 + Y_L^2 R_R L_{\sigma S}^2\right)\omega_e^{*3} - n_p\omega\left(C^2 R_R R_S^2 - \right. \\ &\left. -2CR_R L_{\sigma S} + 2Y_L^2 R_S L_{\sigma R}^2 + 2Y_L L_{\sigma R}^2 + Y_L^2 R_R L_{\sigma S}^2\right)\omega_e^{*2} + \\ &+\left(Y_L R_S + 1\right)\left(R_R + Y_L R_R^2 + \left(n_p\omega\right)^2 L_{\sigma R}^2 Y_L + Y_L R_S R_R\right)\omega_e^* - \\ &-n_p\omega R_R\left(Y_L R_S + 1\right)^2 = 0. \end{aligned} \tag{6}$$

Although up to five solutions are possible, computations with realistic motor parameters typically gives at most one real positive root ω_e^*.

The value of magnetizing inductance is found either from real or imaginary parts of (5). In the first case

$$L_M^* = -c_2 / c_1, \tag{7}$$

where

$$\begin{aligned} c_1 &= -\omega_e^{*2} CR_R - \omega_e^*\left(\omega_e^* - n_p\omega\right)\left(Y_L L_{\sigma S} + Y_L L_{\sigma R} + CR_S\right); \\ c_2 &= R_R\left(1 + Y_L R_S\right) - \omega_e^{*2} CR_R L_{\sigma S} \\ &\quad - \omega_e^*\left(\omega_e^* - n_p\omega\right) L_{\sigma R}\left(Y_L L_{\sigma S} + CR_S\right). \end{aligned}$$

The value of magnetizing current i_M^* is found from the approximation of the experimental dependence in Fig. 1. If $L_M^* > L_{MAX}$ then no solution for i_M^* exists, the self-excitation is impossible. If $L_{M0} < L_M^* < L_{MAX}$, then there are two solutions for i_M^*: the bigger is the stable steady state value, while the smaller determines a critical value to be overcome to trigger the self-excitation via an external energy source (or high enough residual magnetization) and to reach the stable one. If $L_M^* < L_{M0}$, then only one solution exists and it is stable. This operating mode develops naturally due to the instability of the zero state [28].

With $Z^* = \left[U_{SF}^* + jU_{SG}^*, i_{SF}^* + ji_{SG}^*, i_{RF}^* + ji_{RG}^*\right]^T$, the first two rows of (4) accounting the condition $i_M^* = \left|i_S^* + i_R^*\right|$ give the formula for steady-state phase voltage amplitude

$$\left|U_S^*\right| = \frac{\omega_e^* L_M^* i_M^*}{\sqrt{\left(1 + Y_L R_S - C\omega_e^{*2} L_{\sigma s}\right)^2 + \omega_e^{*2}\left(Y_L L_{\sigma s} + CR_S\right)^2}}. \tag{8}$$

The third row of (4) is linearly dependent on the first two rows, due to $\det(F_1^* + jF_2^*) = 0$, and does not give any additional condition.

Finally, the formula for the extracted power is obtained

$$P_L^* = \frac{mY_L\left(\omega_e^* L_M^* i_M^*\right)^2}{2\left(1 + Y_L R_S - C\omega_e^{*2} L_{\sigma s}\right)^2 + \omega_e^{*2}\left(Y_L L_{\sigma s} + CR_S\right)^2}, \tag{9}$$

where m is the number of phases.

Note, that ω is not directly present in (9). However, the generated frequency ω_e^* in (6) depends on all possible control/disturbances inputs ω, Y_L, and C. The magnetizing current and inductance depend on ω_e^*, ω, Y_L, and C. As result, the derivatives $\partial P_L^* / \partial C$, $\partial P_L^* / \partial Y_L$, and $\partial P_L^* / \partial \omega$ can not be found analytically. Therefore, the analytic search for a global maximum point of the function $P_L^* = f\left(\omega, Y_L, C\right)$ is impossible and a numerical approach should be applied.

Consider the most practical case when the velocity of the generator is fixed. Then three-dimensional plots $P_L^* = f\left(Y_L, C\right)$ for fixed values of ω are to be computed for all possible operating points, meaning all operating conditions ω, Y_L, and C which give the solution of (7) $L_M^* < L_{MAX}$. Following the approach from [28] and [30] there is no need to find iteratively the self-excitation boundaries, meaning the conditions where $L_M^* = L_{MAX}$. They are derived eliminating $\omega_e^* - n_p\omega$ from the real and imaginary parts of (5) for a given L_M^*:

$$f_1\omega_e^{*4} + f_2\omega_e^{*2} + f_3 = 0, \quad (10)$$

where

$f_1 = C^2 L_S^* \left(L_S^* L_R^* - L_M^{*2}\right) > 0;$

$f_2 = Y_L^2 L_S^* \left(L_S^* L_R^* - L_M^{*2}\right) + C^2 R_S^2 L_R^* - C\left(2L_S^* L_R^* - L_M^{*2}\right);$

$f_3 = L_R^* \left(Y_L R_S + 1\right)^2 > 0$

with $L_S^* = L_{\sigma S} + L_M^*$, $L_R^* = L_{\sigma R} + L_M^*$ and substitution $L_M^* = L_{MAX}$.

If condition $f_2 < -2\sqrt{f_1 f_3}$ is satisfied, there are two real positive solutions to equation (10) $\omega_{e,\min}^*$ and $\omega_{e,\max}^*$ which determine minimum and maximum possible generated frequencies for given C and Y_L.

The critical velocities $\omega_{\min}$ and $\omega_{\max}$ corresponding $\omega_{e,\min}^*$ and $\omega_{e,\max}^*$ can be found from the real (or imaginary) part of equation (5)

$$\omega = \frac{1}{n_P}\left(\omega_e^* - \frac{Y_L R_S R_R - \omega_e^{*2} C R_R L_S^* + R_R}{\omega_e^*\left(Y_L\left(L_S^* L_R^* - L_M^{*2}\right) + R_S L_R^* C\right)}\right), \quad (11)$$

with substitution $L_M^* = L_{MAX}$, and $\omega_e^* = \omega_{e,\min}^*$ or $\omega_e^* = \omega_{e,\max}^*$ respectively.

The dependences $\omega_{\min} = f(C)$ and $\omega_{\max} = f(C)$ plotted in the $C - \omega$ plane for a given Y_L constitute the self-excitation boundary which contains all possible operating points for this load. For the purpose of the paper, the boundary should be rearranged in the $C - Y_L$ plane for a given ω_e^*.

Alternatively, equation (10) can be presented as a quadratic equation [29]

$$g_1 C^2 - g_2 C + g_3 = 0, \quad (12)$$

where $g_1 = L_S^*(L_S^* L_R^* - L_M^{*2})\omega_e^{*4} + R_S^2 L_R \omega_e^{*2} > 0$;

$g_2 = (2L_S^* L_R^* - L_M^{*2})\omega_e^{*2} > 0$;

$g_3 = Y_L^2(L_S^*(L_S^* L_R^* - L_M^{*2})\omega_e^{*2} + L_R^* R_S^2) + 2L_R^* R_S Y_L + L_R^* > 0.$

The quadratic equation with $L_M^* = L_{MAX}$ has two real positive solutions $C_{\min}$ and $C_{\max}$ if and only if $g_2^2 - 4g_1 g_3 > 0$. Substitution them into equation (11) gives $\omega_{\min}$ and $\omega_{\max}$. The obtained values of capacitances and velocities constitute corresponding critical ranges for given ω_e^* and Y_L.

Another representation of (10) is

$$a_1 Y_L^2 + a_2 Y_L + a_3 = 0, \quad (13)$$

where

$a_1 = L_S^*(L_S^* L_R^* - L_M^{*2})\omega_e^{*2} + L_R^* R_S^2 > 0$; $a_2 = 2L_R^* R_S > 0$;

$a_3 = C^2(L_S^*(L_S^* L_R^* - L_M^{*2})\omega_e^{*4} + R_S^2 L_R^* \omega_e^{*2}) - C(2L_S^* L_R^* - L_M^{*2})\omega_e^{*2} + L_R^*.$

If $a_2^2 - 4a_1 a_3 \geq 0$ is satisfied then one solution of equation (13) is negative, while another solution

$$Y_{L\max} = \left(-a_2 + \sqrt{a_2^2 - 4a_1 a_3}\right)/(2a_1), \quad (14)$$

is positive or zero only if $a_3 \leq 0$.

For given ω_e^* and C, $Y_{L\max}$ and $Y_{L\min} = 0$ constitute the critical range of loads for the self-excitation. The corresponding velocity range is found substituting the critical load admittances into (11).

The self-excitation boundary in the $C - Y_L$ plane can be computed either based on (12) or (14) in the forms $C_{\min} = f(Y_L)$ and $C_{\max} = f(Y_L)$ or $Y_{L\max} = f(C)$ for a given ω_e^*.

The maximum possible load admittance the SEIG can sustain [29], [30] is

$$Y_{LCR} = \frac{(\sqrt{\sigma} - 1)^2}{4R_S\sqrt{\sigma}}, \quad (15)$$

where $\sigma = \left(L_S L_R - L_{MAX}^2\right)/(L_S L_R) > 0$;

$L_S = L_{\sigma S} + L_{MAX}$, $L_R = L_{\sigma R} + L_{MAX}$.

The maximum possible capacitance that can provide self-excitation is for no load case [29]

$$C_{CR} = \frac{2L_S L_R - L_{MAX}^2 - 2\sqrt{L_S L_R (L_S L_R - L_{MAX}^2)}}{R_S^2 L_R}. \quad (16)$$

For a given velocity ω, the value of the extracted power should be computed based on (9) for all operating conditions from 0 to Y_{LCR} and from 0 to C_{CR} and the operating conditions not satisfying the solutions of (12) or (13) must be neglected.

Computations and experiments were done for two different SEIGs: АИРМ63В4У3 (produced in Ukraine), with rated values 370 W, 380 V (Y), 50 Hz, and 1450 rpm, and Bk2208 (produced in UK), with rated values 250 W, 240 V (Δ), 50 Hz, and 1425 rpm.

In the first case, the SEIG was coupled to another induction motor (4AM80B3Y3, with rated values 2.2 KW, 380 V, 50 Hz, and 2800 rpm) controlled through the frequency converter ABB ACS140 feeding the stator windings. The higher value of the motor's power and the slip compensation function in the ACS140 provided velocity stabilization during experiments. The loads were Y-connected. During experiments, the capacitors were Δ-connected, so that the values shown in plots were tripled to correspond to an equivalent Y-connection. Collection of the experimental data was performed using the ACS140's monitoring system and a system for testing of electric drives that provided voltage and current measurements with visualization compatible with Matlab.

In the second case, the experimental rig was similar. The ABB induction motor M3AA090LB-4 (with rated values 1.1 KW, 230 V (Δ), 50 Hz, and 1435 rpm) controlled through the frequency converter ABB ACS355 was used as a prime mover. During experiments, the excitation capacitors and the loads were Y-connected. The proposed analysis combining with equivalent Y to Δ-connection transforms was used for obtaining line-to-line SEIG voltage amplitudes. All the figures were plotted for actual values of the load admittances and capacitances. The line-to-line voltage measurements were taken between all three phases through Hall effect voltage transducers LV25-P and read through dSpace DS1104 analogue-to-digital converters. The velocity of the motor was monitored through A2108 optical tachoprobe.

The following parameters of the generators were determined experimentally: R_S=27 Ω, R_R=17.9 Ω, $L_{\sigma S} = L_{\sigma R}$=0.08266 H, n_p=2 for АИРМ63В4У3, and R_S=31.65 Ω, R_R=28.1 Ω, $L_{\sigma S} = L_{\sigma R}$=0.0921 H, n_p=2 for Bk2208. The analytic approximation of the magnetizing inductance is presented in [31], [32]. The following parameters of the approximation were determined for the АИРМ63В4У3 SEIG based on experiments: p_1=-0.005214 H/A^3, p_2=0.08245 H/A^2, p_3=-0.4811 H/A, p_4=1.226 H, p_5=-0.02035 HA, L_{MAX}=1.031 H, L_{M0}=0.635 H, i_{M1}=0.105 A, i_{M2}=0.213 A, b_1=35.98 H/A^2, i_{M3}=3.042 A, Ψ_{MMAX}=1.130 Wb. In the second case for the Bk2208 SEIG, the parameters were p_1=-0.235 H/A^3, p_2=1.357 H/A^2, p_3=-3.223 H/A, p_4=3.841 H, p_5=-0.3536 HA, L_{MAX}=1.87 H, L_{M0}=1 H, i_{M1}=0.333 A, i_{M2}=0.396 A, b_1=7.8457 H/A^2, i_{M3}=1.738 A, Ψ_{MMAX}=1.5664 Wb.

Figs. 2 and 3 depict the generated power as a function of load admittance and velocity for АИРМ63В4У3. The experimental and computed results are in good agreement.

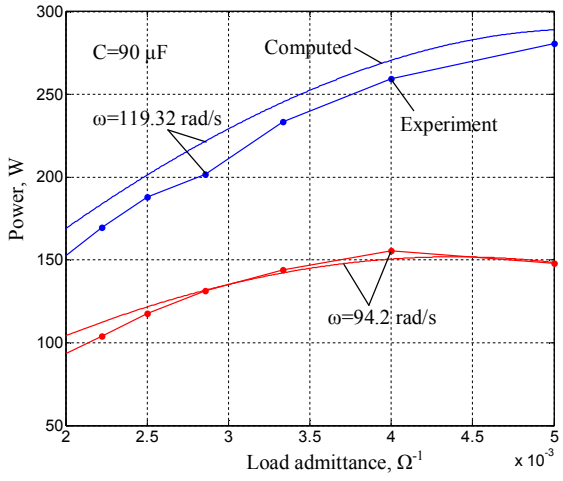

Figure 2 – Steady-state power as a function of the load admittance for different velocities, АИРМ63В4У3

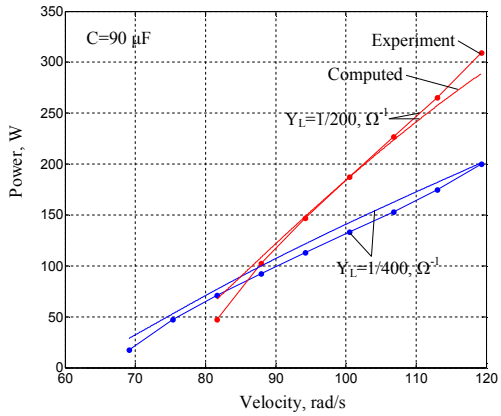

Figure 3 – Steady-state power as a function of the velocity for different loads, АИРМ63В4У3

The 3–D plots computed for АИРМ63В4У3 within the self-excitation boundaries (curve 1 or curve 2 as a 2-D plot) for the extracted power are presented in Figs. 4 and 5. The maximum points belong to curves 3. The computations prove the existence of the operating point with maximum power within the self-excitation boundaries (global maximum).

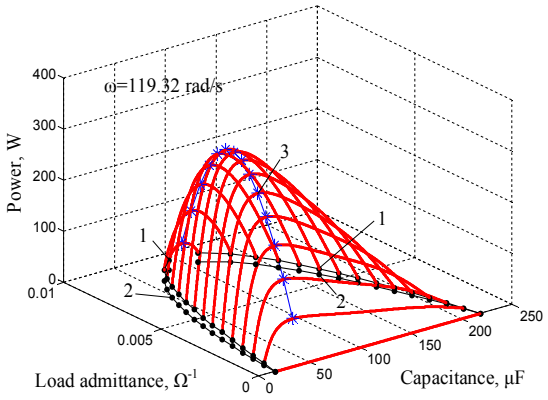

Figure 4 – Steady-state power as a function of capacitance computed through the range of load admittance, АИРМ63В4У3

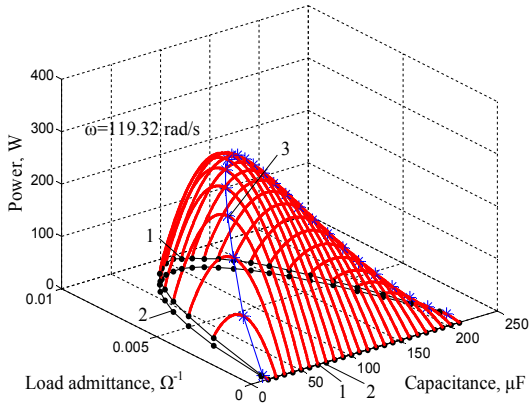

Figure 5 – Steady-state power as a function of the load admittance computed through the range of capacitance, АИРМ63В4У3

Figs. 6–9 show the computed and experimental results for the Bk2208 SEIG which confirm the conclusions made for the АИРМ63В4У3 SEIG.

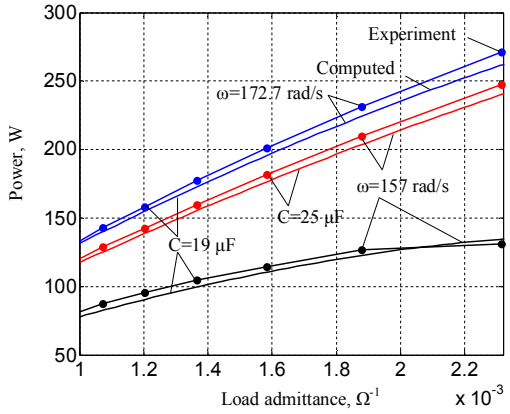

Figure 6 – Steady-state power as a function of the load admittance for different velocities and capacitances, Bk2208

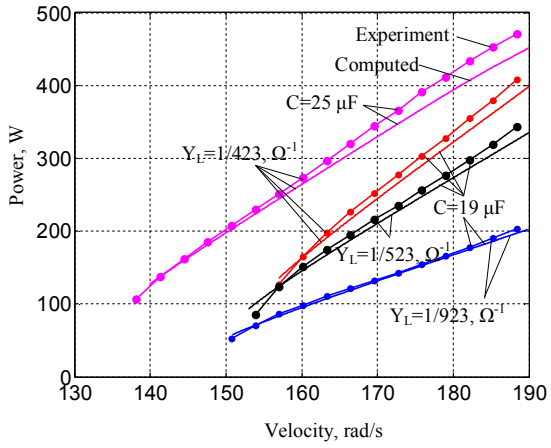

Figure 7 – Steady-state power as a function of the velocity for different loads and capacitances, Bk2208

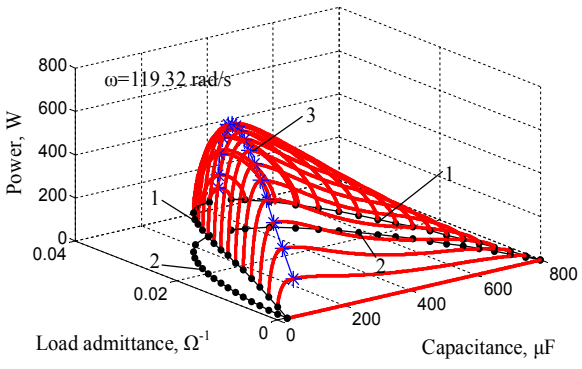

Figure 8 – Steady-state power as a function of capacitance computed through the range of load admittance, Bk2208

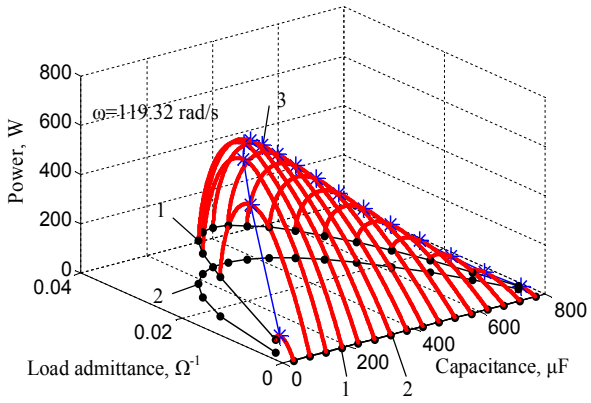

Figure 9 – Steady-state power as a function of the load admittance computed through the range of capacitance, Bk2208

For a specific value of load, a control algorithm can be implemented searching for a capacitance value providing a maximum of the function $P_L^* = f(C)$ or approaching this value. The algorithm is based on switching the capacitance with a fixed step with a sample time sufficient for decay of the transients. Measurements of steady-state power are taken at each sample time. If the difference of two consequent measurements is positive, then the change of the capacitance is kept in the same direction. If the difference becomes negative, then the change of the capacitance is made in the opposite direction. As a result, there appears a sequence of steady states oscillating around the maximum point. The value of the sample time determines the frequency of the oscillations. The value of the capacitance step determines the amplitude of the oscillations and the maximum search time. During the search, some restrictions on the value of the generated voltage can be imposed.

CONCLUSIONS. The paper develops a theory justifying the possible implementation of control systems providing maximum extraction of SEIG power. The results are based on formulas obtained for steady-state power and self-excitation boundaries, and are validated experimentally. They show the existence of the SEIG operating point with a maximum power in the capacitance – load admittance plane for a given velocity. The paper gives insight into the implementation of an algorithm searching for capacitances that provide an operating point with maximum power.

REFERENCES

1. Chauhan, Y.K., Jain, S.K. and Singh, B. (2010), "A prospective on voltage regulation of self-excited induction generators for industry applications," *IEEE Trans. Industry Applications*, Vol. 46, no. 2, pp. 720–730.

2. Chandra Sekhar, T. and Muni, B.P. (2004), "Voltage regulators for self excited induction genera-

tor," *Proc. of IEEE Region 10 Conference TENCON,* Vol. C, pp. 460–463.

3. Touti, E., Pusca, R., Brudny, J.F. and Chaari, A. (2013), "A fuzzy logic and numerical frequency control of a self excited asynchronous generator in remote site," *Proc. of 2013 International Conference on Control, Decision and Information Technologies*, pp. 536–542.

4. Dastagir, G. and Lopes, L.A.C. (2007), "Voltage and Frequency Regulation of a Stand-Alone Self-Excited Induction Generator," *Proc. of IEEE Canada Electrical Power Conference,* pp. 502–506.

5. Ramirez, J.M. and Torres, E. (2007), "An electronic load controller for the self-excited induction generator," *IEEE Trans. Energy Conversion*, Vol. 22, no. 2, pp. 546–548.

6. Singh, B., Murthy, S.S. and Gupta, S. (2005), "Transient analysis of self-excited induction generator with electronic load controller (ELC) supplying static and dynamic loads," *IEEE Trans. Industry Applications,* Vol. 41, № 5, pp. 1194–1204.

7. Bonert, R. and Rajakaruna, S. (1998), "Self-excited induction generator with excellent voltage and frequency control," *IEE Proc.: Generation, Transmission and Distribution,* Vol. 145, № 1, pp. 33–39.

8. Sepsi, D.T. and Jardan, R.K. (2012), "Vector based hysteresis control for self-excited induction generators," *Proc. of 15th International Power Electronics and Motion Control Conference (EPE/PEMC)*, pp. DS2d.9-1–DS2d.9-8.

9. Chtchetinine, O. (1999), "Voltage stabilization system for induction generator in stand alone mode," *IEEE Trans. Energy Conversion*, Vol. 14, № 3, pp. 298–303.

10. Geng, Hua, Xu, D., Wu, Bin and Huang, Wei (2011), "Direct voltage control for a stand-alone wind-driven self-excited induction generator with improved power quality", *IEEE Trans. Power Electronics,* Vol. 26, № 8, pp. 2358–2368.

11. Louze, L., Memmour, A.L., Khezzar, A. and Boucherma, M. (2009), "Input-output linearizing and sliding mode control schemes for a self-excited induction generator," *Proc. of 35th Annual Conference of IEEE Industrial Electronics,* pp. 3892–3897.

12. Chen, W.-L., Lin, Y.-Hs., Gau, H.-S. and Yu, C.-H. (2008), "STATCOM controls for a self-excited induction generator feeding random loads," *IEEE Trans. Power Delivery,* Vol. 23, № 4, pp. 2207–2215.

13. Chatterjee, J.K., Perumal, B.V. and Gopu, N.R. (2006), "Analysis of operation of a self-excited induction generator with generalized impedance controller", *IEEE Trans. Energy Conversion,* Vol. 22, no. 2, pp. 307–315.

14. Singh, B., Murthy, S.S. and Gupta, S. (2006), "STATCOM-based voltage regulator for self-excited induction generator feeding nonlinear loads," *IEEE Trans. Ind. Electron,* Vol. 53, no. 5, pp. 1437–1452.

15. Chan T.F. (1995) "Analysis of self-excited induction generators using an iterative method," *IEEE Trans. Energy Conversion*, Vol. 10, no. 3, pp. 502–507.

16. Biglari, A. and Miraftabi, S.A. (2012), "Steady-state analysis and voltage control of self-excited induction generator (SEIG)," *Proc. of 11th International Conference on Environment and Electrical Engineering (EEEIC)*, pp. 776–781.

17. Malik, N.H. and Haque, S.E. (1986), "Steady state analysis and performance of an isolated self-excited induction generator," *IEEE Trans. Energy Conversion,* Vol. EC–1, no. 3, pp. 134–140.

18. Murthy, S.S., Malik, O.P. and Tandon, A.K. (1982), "Analysis of self-excited induction generators", *IEE Proc.*, Vol. 129, pt. C, no. 6, pp. 260–265.

19. Grantham, C., Sutanto, D. and Mismail, B. (1989), "Steady-state and transient analysis of self-excited induction generators," *IEE Proc.*, vol. 136, pt. B, no. 2, pp. 61–68.

20. Malik, N.H. and Al-Bahrani, A.K. (1990), "Influence of the terminal capacitor on the performance characteristics of a self excited induction generator," *IEE Proc.,* Vol. 137, no. 2, pp. 168–173.

21. Tandon, A.K., Murthy, S.S. and Berg, G.J. (1984), "Steady-state analysis of capacitor self-excited induction generators," *IEEE Trans. Power Apparatus and Systems*, Vol. 103, no. 3, pp. 612–618.

22. Elder, J.M., Boys, J.B. and Woodward, J.L. (1984), "Self-excited induction machine as a small low-cost generator," *IEE Proc.*, Vol. 131, pt. C, no. 2, pp. 33–41.

23. Alghuwainem, S.M. (1999), "Steady-state analysis of an isolated self-excited induction generator driven by regulated and unregulated turbine", *IEEE Trans. Energy Conversion*, Vol. 14, no. 3, pp. 718–723.

24. Al Jabri, A.K. and Alolah, A.I. (1990), "Capacitance requirement for isolated self-excited induction generator", *IEE Proc. Electric Power Applications,* Vol. 137, pt. B, no. 3, pp. 154–159.

25. Chan, T.F. (1993), "Capacitance requirements of self-excited induction generators," *IEEE Trans. Energy Conversion*, Vol. 8, no. 2, pp. 304–311.

26. Ojo, O. (1995), "Minimum airgap flux linkage requirement for self-excitation in stand-alone induction generators," *IEEE Trans. Energy Conversion*, Vol. 10, no. 3, pp. 484–492.

27. Kuo, S.-C. and Wang, L. (2001), "Dynamic eigenvalue analysis of a self-excited induction generator feeding an induction motor," *Winter Meeting of the IEEE Power Engineering Society*, Vol. 3, pp. 1393–1397.

28. Bodson, M. and Kiselychnyk, O. (2012), "Analysis of triggered self-excitation in induction generators and experimental validation," *IEEE Trans. Energy Conversion,* Vol. 27, № 2, pp. 238–249.

29. Kiselychnyk, O., Pushkar, M. and Bodson, M. (2011), "Critical load of self-excited induction generators," *Electrotechnic and Computer Systems,* Vol. 3, no. 79, pp. 282–285.

30. Bodson, M. and Kiselychnyk, O. (2013), "The complex Hurwitz test for the analysis of spontaneous self-excitation in induction generators," *IEEE Trans. Automatic Control*, Vol. 58, № 2, pp. 449–454.

31. Bodson, M., Kiselychnyk, O. and Wang, J. (2013), "Comparison of two magnetic saturation models of induction machines," *Proc. of 2013 IEEE International Electric Machines & Drives Conference,* Chicago, IL, USA, pp.1004–1009.

32. Kiselychnyk, O., Bodson, M. and Wang, J. (2013), "Model of a self-excited induction generator for the design of capacitor-controlled voltage regulators", *Proc. of 21-st IEEE Mediterranean Conference on Control and Automation*, Crete, Greece, pp. 149–154.

ГЕНЕРИРОВАНИЕ МАКСИМАЛЬНОЙ МОЩНОСТИ АСИНХРОННЫХ ГЕНЕРАТОРОВ С САМОВОЗБУЖДЕНИЕМ

О. И. Киселичник, Дж. Вонг
Университет Ворвика
Ковентри, CV4 7AL, Великобритания. E-mail: O.Kiselychnyk@warwick.ac.uk, jihong.wang@warwick.ac.uk
М. Бодсон
Университет Юты
Солт Лейк Сити, UT 84112, США. E-mail: bodson@eng.utah.edu
Н. В. Пушкарь
Национальный технический университет Украины "Киевский политехнический институт"
просп. Победы, 37, м. Киев, 03056, Украина. E-mail: pushkar.mykola@gmail.com

Способы управления напряжением асинхронных генераторов с самовозбуждением могут быть использованы для максимизации мощности отдельных применений, которые не имеют жестких требований к генерируемой частоте и напряжению. Основной проблемой разработки таких систем является отсутствие соответствующих теоретических основ. В данной работе рассматривается подход к максимизации генерируемой мощности асинхронных генераторов с самовозбуждением. Выводятся формулы для статической мощности генератора и границ самовозбуждения. Поскольку аналитическое исследование зависимости мощности от емкости конденсаторов и проводимости нагрузки на экстремум оказывается невозможным, то применяется численный метод, который включает построение трехмерных расчетных и двухмерных экспериментальных характеристик, которые доказывают существование точки глобального максимума мощности в пределах границы самовозбуждения для соответствующей скорости, построенной в плоскости емкость–проводимость нагрузки. Таким образом, данный метод позволяет учесть все возможные рабочие точки генератора для заданной скорости. Дискутируются вопросы реализации алгоритмов поиска точки максимума мощности.

Ключевые слова: асинхронный генератор, самовозбуждение, максимальная выходная мощность, статические характеристики мощности.

Стаття надійшла 13.05.2014.